J. Fluid Mech. (1964), *vol.* 20, *part* 4, *pp.* 555–579
Printed in Great Britain

The wall-jet in a moving stream

By V. KRUKA AND S. ESKINAZI
Mechanical Engineering Department, Syracuse University, Syracuse 10, New York

(Received 25 September 1963 and in revised form 7 April 1964)

1. Introduction

The wall-jet is the flow of fluid emanating from a narrow slot and blowing over a rigid wall. The configuration of the turbulent wall-jet is that of a very narrow, plane, turbulent half-jet investigated by Liepmann & Laufer (1947). The width of the slot is of the order of the boundary layer on the infinite wall and the jet, in this case, mixes with a stream moving with constant velocity. This flow has drawn considerable basic and applied interest in the past few years for it has the characteristics of both a boundary-layer and a free-mixing flow.

The similarity solution approach to boundary-value problems in fluid mechanics has been useful. This approach has been effectively used by Glauert (1956) for the solution of the wall-jet in a still medium. Based on physical reasoning he was the first to postulate that, in a strict sense, the entire flow of the wall-jet cannot conform to one overall similarity solution. He divided the flow into an inner and outer portion on either side of the maximum velocity and treated the two regions separately. Eichelbrenner & Dumargue (1962) treated the plane, turbulent wall-jet in a moving stream of constant velocity. They also separated the flow into two regions; Glauert's solution for the inner profile and Görtler's solution of the mixing of two parallel streams for the outer profile. However, the point of joining occurs between the maximum velocity and the inflexion point in the outer profile, thereby avoiding Glauert's discontinuity in the eddy viscosity.

The present experimental investigation of a plane, steady, turbulent wall-jet with negligible longitudinal pressure gradients in a constant moving stream, with varying ratios of jet to free-stream velocity definitely supports Glauert's reasoning, though the precise point of partition of the flow might be in question. The inner layer is constantly losing momentum due to the frictional stresses at the wall, while the outer layer tends to preserve its momentum; the division now occurring at the point of zero shear which may not coincide with the location of maximum velocity. This separation of null shears was first pointed out by Eskinazi & Yeh (1956) who showed that for asymmetrical velocity profiles the zero value of the fluctuating velocity correlation $\overline{uv}$ was not at the point of maximum velocity. For the wall-jet this phenomena was indicated by Mathieu (1959) and is definitely shown by the present data.

Patel & Newman (1961), in working with the wall-jet in a moving stream, defined and supported a simple set of similarity functions for the mean and turbulent flow which were found not to be very agreeable with our experiments. Under these conditions they concluded analytical similarity to be possible only if the ratio of maximum excess to free-stream velocity remained constant.

The analysis and experimental results are compared with those of previous investigators and a definite comparison of this work with those performed in a quiescent free stream is achieved through transformation of co-ordinates.

2. Analytical considerations

In most boundary-layer and free-mixing problems the existence of a dimensionless similarity function $f(\eta)$ in the velocity field, where η is the transverse distance made dimensionless with a x-dependent characteristic dimension, usually reduces the Prandtl-type partial differential equation of motion to a dimensionless total differential equation. The coefficients of this equation are constant provided the similarity function $f(\eta)$ is postulated to be independent of the history of the flow (x in the steady case). In boundary-layer flows the free-stream velocity and the boundary-layer thickness are found to be suitable characteristic quantities, while in free-mixing flows the maximum velocity at any longitudinal section and the corresponding half-width of the jet or wake are adequate. In the analytical treatment, for similar solutions to exist, the substitution of $f(\eta)$ in the dynamical equations must yield a differential equation in f that is completely independent of x. The coefficients of this equation must then also be constant with x and thus give additional relations between various flow properties for which this 'analytical similarity', as we shall call it, must exist. Experimental results are usually valuable in establishing the definition of the similarity function and its variable. This does not imply, however, that in general the definition of η and $f(\eta)$ thus obtained and which yields an apparent 'experimental similarity' will also yield analytical similarity, or vice-versa. The reason for introducing these two different similitudes is that the form of the similarity function which will satisfy experiment and analysis is not always apparent. In the absence of longitudinal pressure gradients many authors, including the present ones, have found very convincing experimental similitude not only in the confines of their own experiments but, as it will be shown in this paper, also for varying ratios of free stream to jet velocities.

As mentioned previously, Glauert as well as Eichelbrenner & Dumargue showed that strictly speaking there cannot be a general similarity for the entire wall-jet. This was verified conclusively by the experiments of the authors (1962*a*). The flow is divided into two regions separated by the position at which the correlation $\overline{uv} = 0$. However, since the determination of this position is impractical for mean velocity considerations, the location of the maximum velocity is chosen as the dividing point. The region from the wall to the maximum velocity will be referred to as the inner or wall region and that from the maximum velocity point to the beginning of the free stream as the outer or free-mixing region.

(*a*) *Similarity in the wall region*

Figure 1 shows that, in the wall region, there is a fair experimental similarity in the temporal mean velocity for the free stream to jet velocity ratio $\beta = 0{\cdot}100$. The similarity transformation variable is defined as y/δ_1 and the similarity function $f(\eta)$ as U/U_m. For definition of terms see figure 2 which describes the

geometry of the flow. The effects of different β's on $f(\eta)$ will be discussed later. The Reynolds equation in the longitudinal direction for zero pressure gradient is given by

$$U\frac{\partial U}{\partial x}+V\frac{\partial U}{\partial y}+\frac{\partial}{\partial x}(\overline{u}^2-\overline{v}^2)=\frac{1}{\rho}\frac{\partial \tau}{\partial y}=\frac{\partial U_*^2}{\partial y}, \tag{1}$$

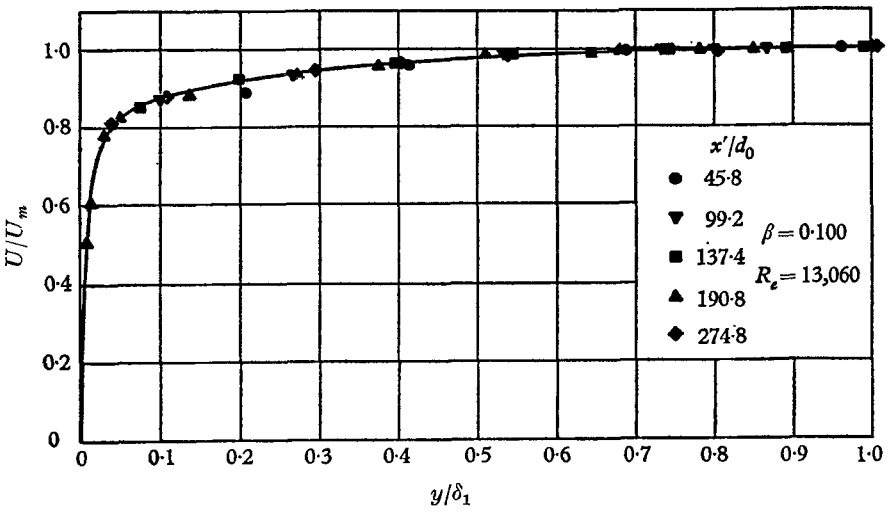

FIGURE 1. Non-dimensional velocity profile in the wall region.

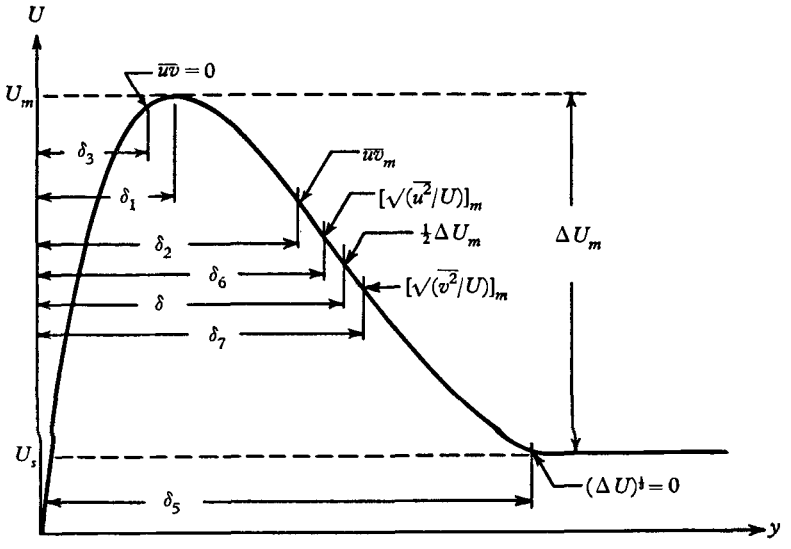

FIGURE 2. Velocity profile and its geometry.

where U and V are the temporal mean velocities in the longitudinal and lateral directions, respectively, u and v the corresponding fluctuating components, τ the total shear stress, U_* the shearing velocity and x the longitudinal distance from the virtual origin x_0. Near the wall the contribution of the difference in the normal Reynolds stresses is small compared with the other terms and will be neglected.

Substituting the quantities η and $f(\eta)$ in the continuity equation and integrating for V one obtains

$$V = -\frac{d}{dx}(\delta_1 U_m)\int_0^\eta f(\zeta)\,d\zeta + U_m \frac{d\delta_1}{dx}\eta f(\eta). \tag{2}$$

Finally, using (2) and the similarity definitions in (1), the simplified Reynolds equation becomes

$$U_m \frac{dU_m}{dx} f^2(\eta) - \frac{U_m}{\delta_1}\frac{d}{dx}(\delta_1 U_m) f'(\eta)\int_0^\eta f(\zeta)\,d\zeta = \delta_1^{-1}\frac{\partial U_*^2}{\partial \eta}. \tag{3}$$

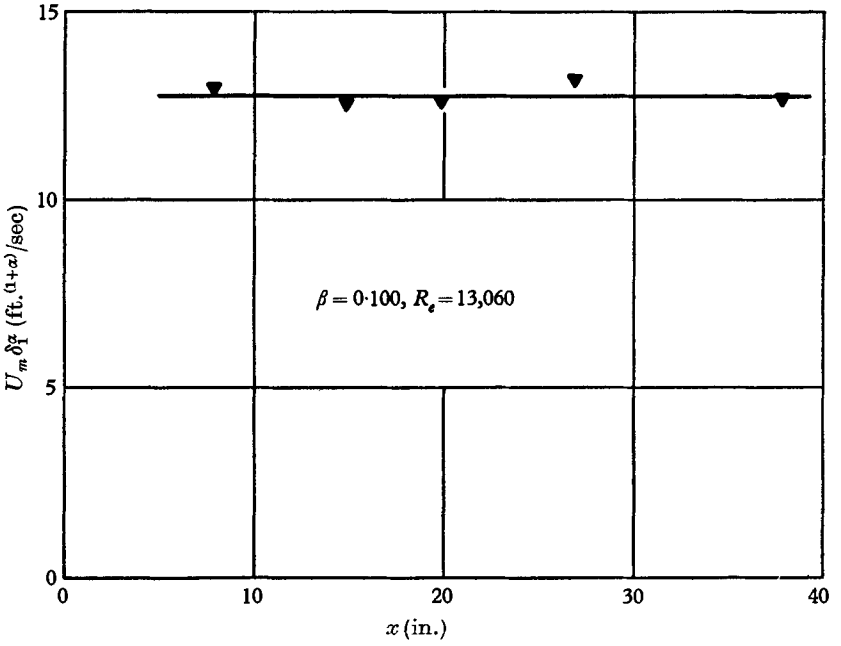

FIGURE 3. Similarity condition in the wall region.

Division of (3) by the first-dimensional coefficient yields

$$f^2(\eta) - \left(\frac{U_m}{\delta_1}\frac{d\delta_1}{dU_m} + 1\right) f'(\eta)\int_0^\eta f(\zeta)\,d\zeta = 2\delta_1^{-1}\frac{\partial U_*^2}{\partial \eta}\Big/\frac{dU_m^2}{dx}. \tag{4}$$

For $f(\eta)$ in (4) to be a unique, similar solution of one variable η representing the entire inner flow, its functional must be independent of x and y. Hence all the coefficients of f and functions of f must be proportional. Thus

$$-\left(1 + \frac{U_m}{\delta_1}\frac{d\delta_1}{dU_m}\right) = k.$$

The solution of this equation yields

$$U_m \delta_1^\alpha = c_0, \tag{5}$$

where $\alpha = (1+k)^{-1}$.

This is found to be true experimentally for each β in figure 3, however, with α being a function of β.

As in the case of the boundary layer, the experiments of Patel (1962) and Schwarz & Cosart (1961) showed that $f(\eta)$ can be represented as $\eta^{1/n}$ with $n = 11{\cdot}0$ and $14{\cdot}0$, respectively. The present work indicates that

$$f(\eta) = 1{\cdot}03\eta^{1/n}$$

accurately describes the data for values of η up to $0{\cdot}7$, however, with the values of n varying with β: for $\beta = 0{\cdot}263$, $n = 10{\cdot}3$; $\beta = 0{\cdot}100$, $n = 13{\cdot}4$; $\beta = 0{\cdot}055$, $n = 12{\cdot}3$. Although n was found to vary by about 30 % the value of the integral of the velocity profiles varied slightly if taken up to $y = \delta_3$, the point at which the shear is zero.

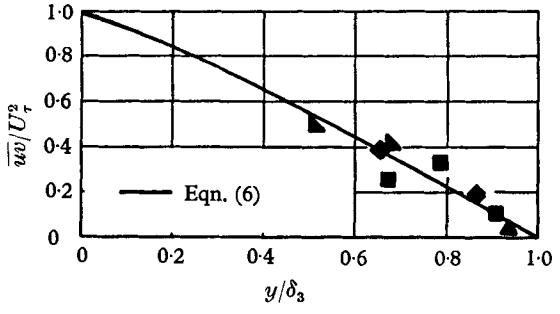

FIGURE 4. Non-dimensional shear profile in the wall region.

Substituting the expression for $f(\eta)$ in (4) leads to

$$\frac{2}{\delta_1}\frac{\partial U_*^2}{\partial \eta} = (1{\cdot}03)^2\left(1+\frac{\alpha^{-1}-1}{n+1}\right)\eta^{2/n}\frac{dU_m^2}{dx},$$

which upon integration with respect to y yields

$$U_*^2(y) - U_\tau^2 = \frac{(1{\cdot}03)^2}{2(2/n+1)}\left(1+\frac{\alpha^{-1}-1}{n+1}\right)\frac{dU_m^2}{dx}\frac{y^{(2/n)+1}}{\delta_1^{2/n}}$$

where U_τ designates the wall shearing velocity. Use of the condition $U_*^2 = 0$ at $y = \delta_3$ in the above relation leads to

$$U_*^2(y) = U_\tau^2[1-(y/\delta_3)^{(1+2/n)}]. \tag{6}$$

This relation between U_*^2 and y in the wall region is supported experimentally as shown in figure 4.

To obtain the wall shear an integration for the entire flow is usually performed; however, since the contribution from the free stream to $y = \delta_3$ is zero, only the inner portion needs to be considered. The integration of (3) from $y = 0$ to $y = \delta_3$, or from $\eta = 0$ to $\eta = \eta_3$, then yields the wall shear in the form

$$U_\tau^2 = U_m\frac{d}{dx}(\delta_1 U_m)f(\eta_3)\int_0^{\eta_3} f(\zeta)\,d\zeta - \frac{d}{dx}(\delta_1 U_m^2)\int_0^{\eta_3} f^2(\zeta)\,d\zeta. \tag{7}$$

Due to (5) and the values of α listed on figure 8 the second term on the right-hand side of the equality sign is small compared to the first. If the wall shear is sought from one similarity function for the whole flow then, since η_3 must be replaced by infinity and $f(\infty) = 0$, the second term to the right of (7) is all that remains in the

shear equation. Therefore it stands to reason that the wall shear obtained from an overall similarity function, satisfying the free-mixing flow as well, will yield incorrect results. Letting

$$\phi = f(\eta_3)\int_0^{\eta_3} f(\zeta)\,d\zeta, \quad \text{and} \quad \psi = \int_0^{\eta_3} f^2(\zeta)\,d\zeta,$$

and introducing (5) in (7),

$$U_\tau^2 = c_0^2 \delta_1^{-2\alpha} \frac{d\delta_1}{dx}[\alpha\psi + (\phi - \psi)(1-\alpha)].$$

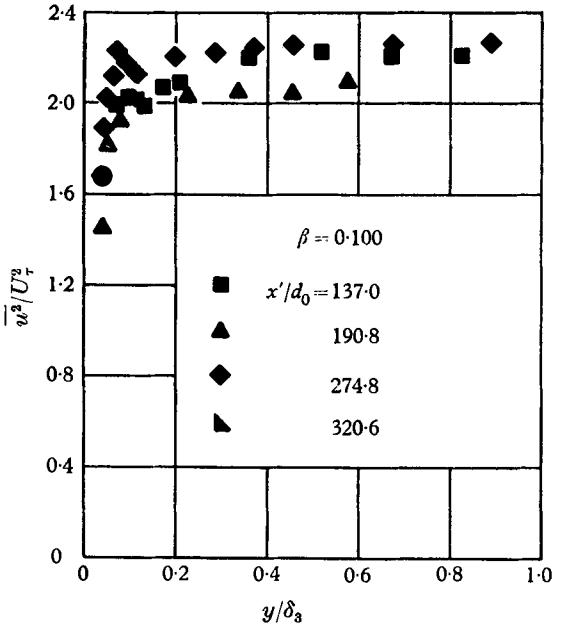

FIGURE 5. Turbulence similarity in the wall region.

For all values of β of the present and many other investigations, figure 6 gives

$$\delta_1 = cx, \tag{8}$$

where $c = 0{\cdot}0109$. Hence

$$U_m = c_1 x^{-\alpha}, \tag{9}$$

which is verified experimentally with fair agreement in figure 8. Use of the above two relations in the expression for wall shear leads to

$$U_\tau^2 = cc_1^2 x^{-2\alpha}[\alpha\psi + (\phi - \psi)(1-\alpha)], \tag{10}$$

where the second term in the brackets is of second order compared to $\alpha\psi$. In the form of the friction coefficient $c_f = 2\tau_w/\rho U_m^2$, where τ_w is the wall shear, (10) reads

$$c_f = 2c[\alpha\psi + (\phi - \psi)(1-\alpha)]. \tag{11}$$

Mathieu (1961) describes a very similar approach for the evaluation of c_f. Experimental verification of the above two equations will be described later.

(*b*) *Similarity in the free-mixing region*

Since the behaviour of wall-jets with and without free streams is unified in this paper, the following relative concept of mixing history is found to be necessary for the correlation of all results. For the longitudinal distances considered the major portion of the flow consists of the free-mixing region. The fact that a free

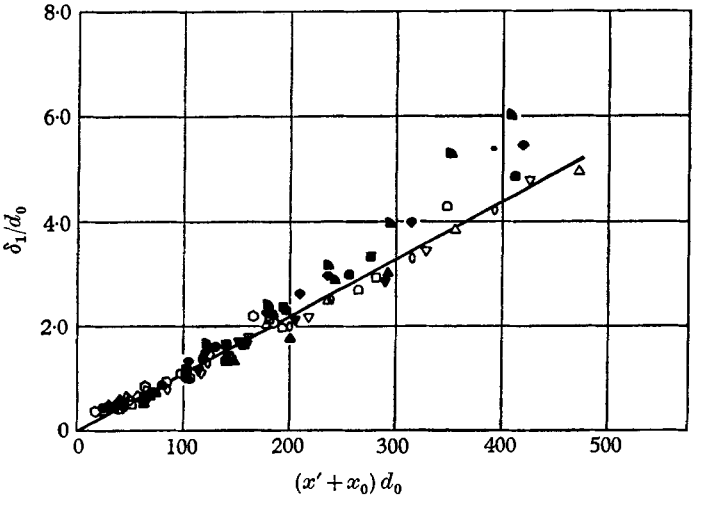

FIGURE 6. Growth on a characteristic width in the wall region.

β	R_e	β	R_e	β	
▲ 0·055	26,270	● 0·485	3,750	◠ 0·190	Verhoff (1963)
▼ 0·100	13,060	◇ 0·386		● 0	Verhoff (1963)
▽ 0·100	11,420	◣ 0·333	Patel (1962)	◗ 0·170	George (1959)
□ 0·263	10,740	◺ 0·168		○ 0·125	Thomas (1962)
■ 0·263	5,790	▲ 0		◖ 0	Mathieu *et al.* (1961)
△ 0·274	8,420	◗ 0·082	Verhoff (1963)	◇ 0	Myers *et al.* (1961).

stream with low turbulence is present suggests that the outer flow in the wall-jet must be viewed as a motion relative to that of the free stream. An infinitesimal longitudinal distance travelled by the fluid relative to the stationary wall is

$$dx' = U\,dt = (U_s + \Delta U)\,dt.$$

The distance travelled by the same particle relative to the free stream is

$$dx_s = \Delta U\,dt.$$

Hence the transformation of these co-ordinate differentials is given by

$$dx'/dx_s = 1 + U_s/\Delta U. \tag{12}$$

Patel & Newman (1961) have shown for the case of a wall-jet with a free stream and Schwarz & Cosart (1961) for the case of no free stream that analytical similarity predicts the excess velocity to decay as the longitudinal distance raised to a power. The present experiments shown in figure 9 verify this power law. Then

$$\Delta U = c_3 x_s^a. \tag{13}$$

Now

$$dx' = 1 + (U_s/c_3 x_s^a)\,dx_s,$$

and integrating from a virtual origin $x' = -x_0$ corresponding to $x_s = 0$, the transformation of the longitudinal co-ordinate becomes

$$x_s = \frac{x' + x_0}{1 + U_s/[(1-a)\,c_3 x_s^a]} = \frac{x}{1 + U_s/[(1-a)\,c_3 x_s^a]}.$$

If one chooses a characteristic value of c_3 obtained from the velocity maximum then the previous transformation becomes

$$x_s = \frac{x}{1 + U_s/[(1-a)\,\Delta U_m]}. \tag{14}$$

This is the basic transformation equation in the outer region. In the case of no free stream, $U_s = 0$, the relative length scale x_s reduces to the actual longitudinal distance x measured from a virtual origin x_0 which is characteristic of free-mixing flows (see, for instance, Townsend 1956). It is found, as shown in figure 9, that the exponent a is constant with x_s for a given ratio of free stream to jet velocity

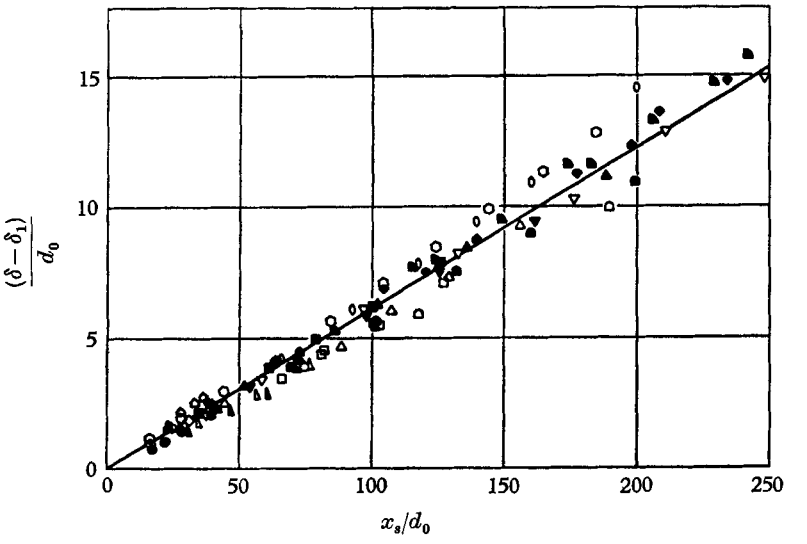

FIGURE 7. Growth of a characteristic width in the free-mixing region.

and furthermore that its variation with Reynolds number, if any, is minimal. This exponent is found to decrease with β. The remarkable usefulness of x_s in correlating characteristic dimensions at various β was already shown by the authors (1962*a*). Figure 7, where the characteristic width of the free-mixing flow $(\delta - \delta_1)$ is shown to fall under one relationship for different values of β and various investigations, further indicates the merits of this reduced co-ordinate. Thus from experimental evidence

$$(\delta - \delta_1) = c_4 x_s, \tag{15}$$

where $c_4 = 0{\cdot}0601$.

Patel & Newman (1961) and others have derived this relation by assuming analytical similarity for the entire flow. It should be emphasized here that for $\beta \neq 0$ and zero pressure gradients, $(\delta - \delta_1)$ is neither a linear nor a unique function of x.

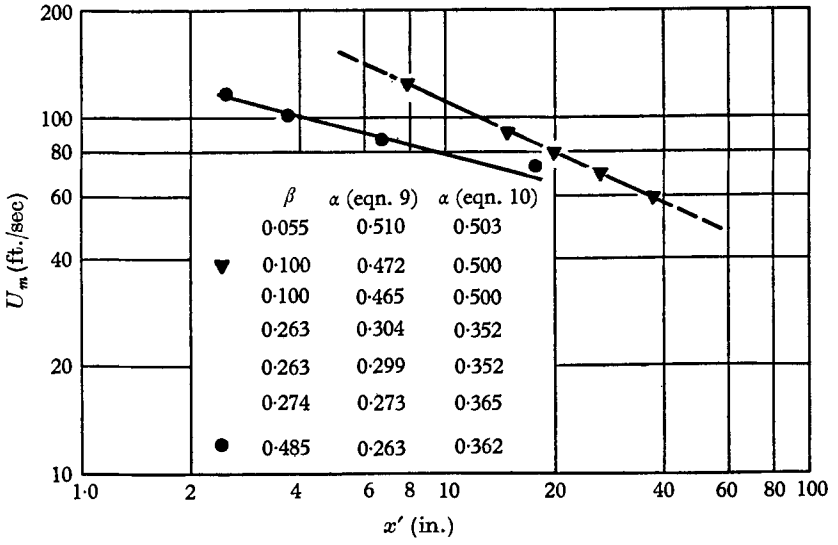

FIGURE 8. Decay of maximum velocity.

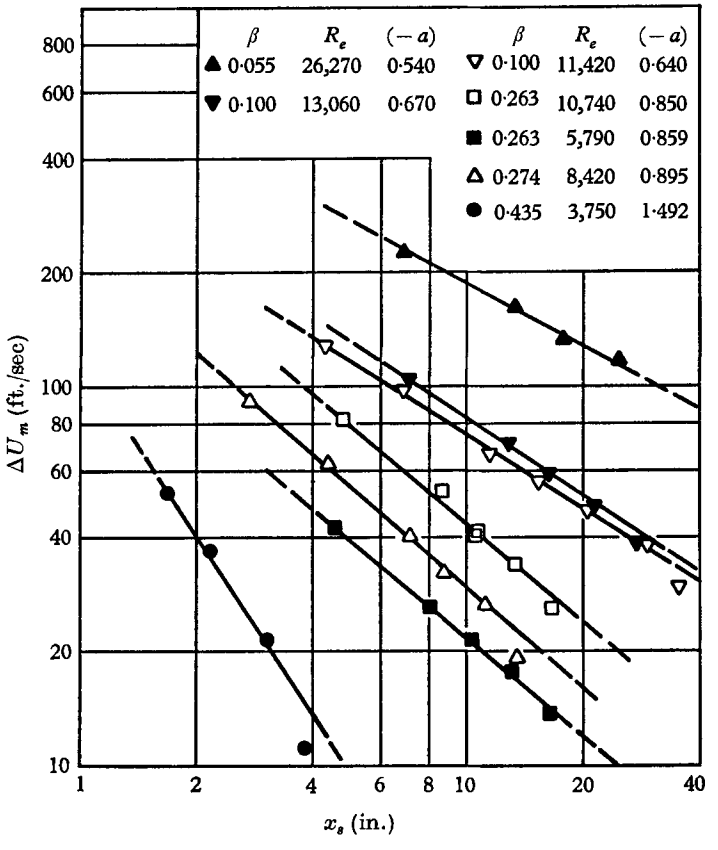

FIGURE 9. Decay of maximum excess velocity.

When similarity is sought for the velocity in the free mixing region with β non-zero, the relative velocity $\Delta U = U - U_s$ must be considered. Figure 9 has already shown that a unique relationship exists between ΔU_m and x_s. This relation is that of (13). However, the figure also shows that the coefficient is a function of the

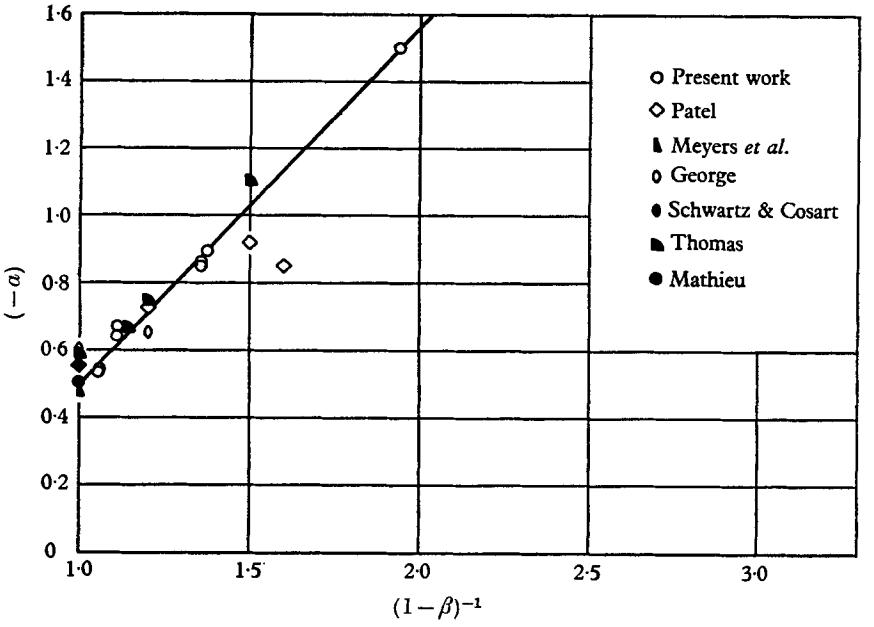

FIGURE 10. Decay exponent of excess velocity.

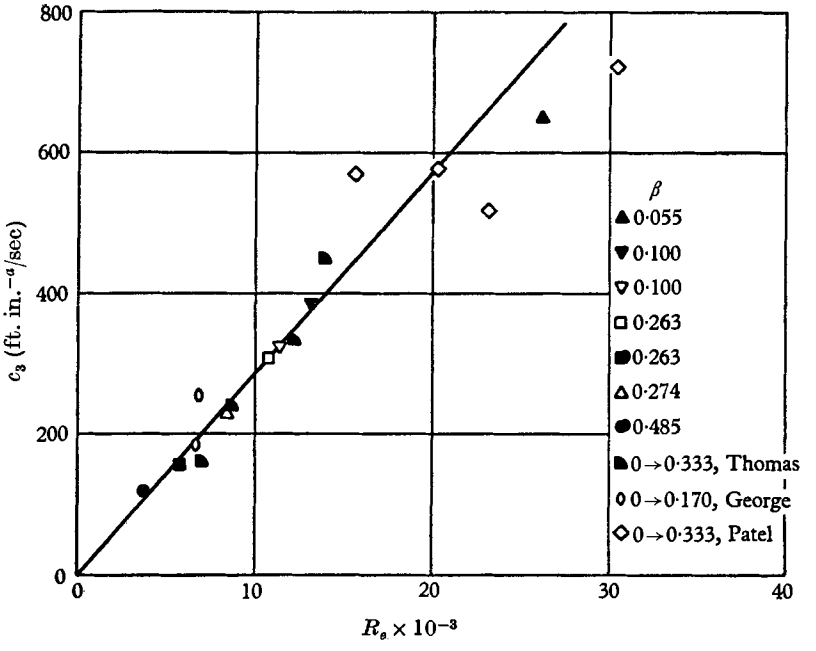

FIGURE 11. Coefficient in (13).

exit Reynolds number R_e, while the exponent a is a function of the velocity ratio β. Figure 10, showing the exponents for all the present experiments together with those of previous investigators, suggests that

$$a = 1{\cdot}06(1-\beta)^{-1} - 0{\cdot}50, \tag{16}$$

while figure 11 indicates that

$$c_3 = 0{\cdot}0287(U_0 d_0/\nu), \tag{17}$$

where $U_0 = U_j - U_s$ is the excess velocity at the jet exit, d_0 is the slot width, ν the kinematic viscosity and c_3 is given in units of ft. (in.)^a/sec. From these relations it is evident that

$$\Delta U_m/U_0 = (0{\cdot}0287/\nu)\, d_0 x_s^a. \tag{18}$$

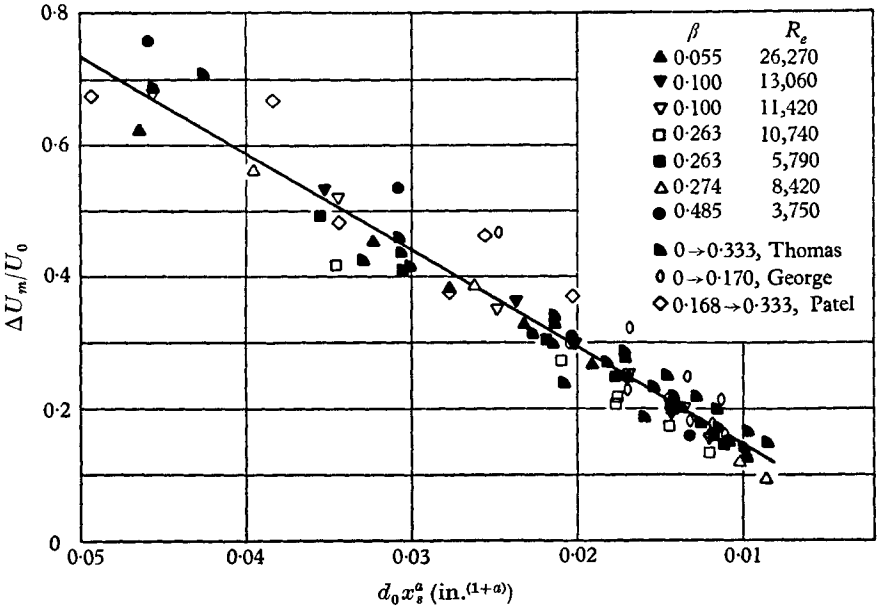

FIGURE 12. Unified decay of maximum excess velocity.

For all values of β previously displayed in figure 9, the present experiments and those of Patel (1962), George (1959) and Thomas (1962) are shown to collapse into the single relation of (18) as shown in figure 12.

Since the decay of the maximum excess velocity has been found as a function of distance, the outer flow suggests a similarity function for the temporal mean velocity of the same form as in the usual free-mixing flows

$$\Delta U/\Delta U_m = F(\xi), \tag{19}$$

where the reduced, dimensionless variable ξ is $(y-\delta_1)/(\delta-\delta_1)$. The velocity then can be expressed as

$$U = \Delta U_m F(\xi) + U_s, \tag{20}$$

where in the present experiments U_s is constant with x but varies in value for different β's. This similarity transformation is shown in figure 13 to agree well

with the experimental results of the outer flow for many values of β. In fact, for $\beta = 0$ it reduces to the well-known similarity form of simple jets and wakes. One disadvantage of this relation is that it brings considerable restrictions in satisfying analytical similarity. If one follows the procedure described for obtaining analytical similarity in the inner flow and substitutes (20) in the Reynolds equation, one immediately sees that the first inertia term $U\partial U/\partial x$ gives

$$[\Delta U_m F(\xi) + U_s]\left\{F(\xi)\frac{d\Delta U_m}{dx} - \frac{\Delta U_m F'(\xi)}{\delta - \delta_1}\left[\frac{d\delta_1}{dx} + \xi\frac{d(\delta-\delta_1)}{dx}\right]\right\}.$$

After expansion of the above relation, the coefficients of $F(\xi)$, $F'(\xi)$ and ξ or any product of them must depend on x in the same manner for the concept of similarity to hold. It is apparent then that the two quantities ΔU_m and U_s in the first bracket must be proportional to each other. This is the restriction Patel & Newman (1961) have followed in their investigation and which is shown in our

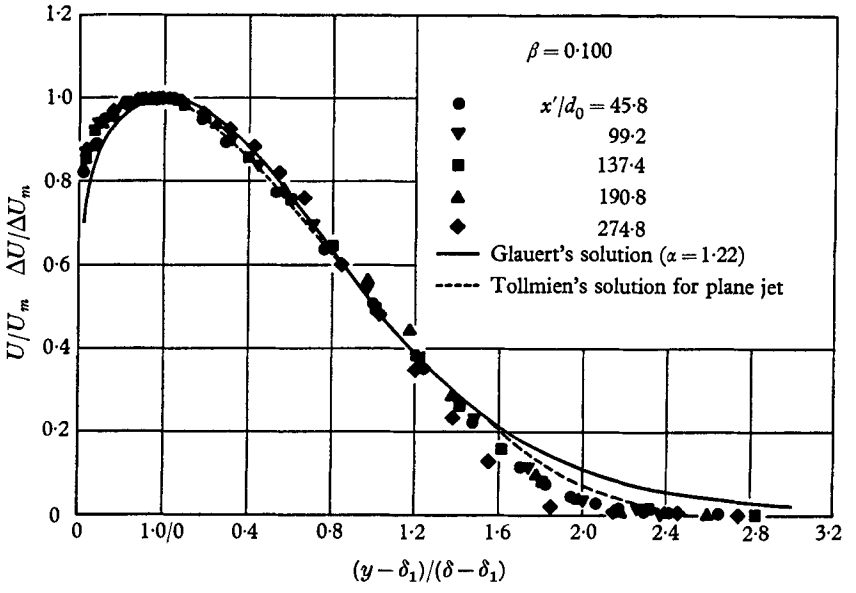

FIGURE 13. Non-dimensional velocity profile.

experiments to be unnecessary for similarity to exist. This conflict between the conditions for analytical and experimental similarity for the case of a constant free stream can only be resolved by the fact that (20) is one restrictive form of the general velocity similarity function. The fact that (20) agrees well with experimental mean velocity should be considered as a fair approximation. However, no inference should be made that there does not exist a more general form of (20) that satisfies both experimental and analytical similarity. All experimental results of the mean and turbulent quantities point to the existence of similarity in the free-mixing region of the flow.

3. Experimental method

(*a*) *Wind tunnel*

The present investigation was conducted in a plane wall-jet blowing tangentially to a semi-infinite, rigid wall and under a uniform moving free stream. The volume rate of air supplied to the wall-jet and that supplied to the free stream was controlled independently to give values of the velocity ratio β of 0·485, 0·274, 0·263, 0·100 and 0·055. For large values of β it was found that at the origin of the mixing

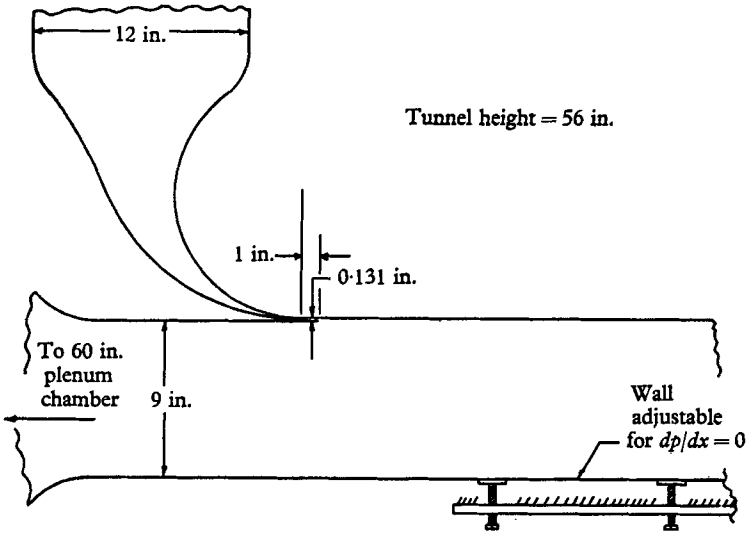

FIGURE 14. Schematic representation of wall-jet.

a temperature difference of as much as 20 °F could occur between the jet and free-stream flows. This, of course, would cause density effects that could not be ignored in the interpretation of the results. Hence the wall-jet was passed through a cooling system in order to remove the frictional heat due to the blower and settling chamber. A second important feature that was resolved in the design of the tunnel was the tolerance in the two-dimensionality of the slot. Those who have worked with plane jets know that a small percentage variation in the two-dimensionality at the jet exit magnifies in the downstream direction to undesirable levels. In this investigation the slot width was 0·131 in. with a maximum variation of one percent throughout its entire height of 56 in. This tolerance was obtained by having the entire nozzle system cast out of steel-kirksite and handworked to the desired dimensions. The width of the free stream was 9·0 in. running the entire height of the jet slot. Figure 14 shows a sketch of the tunnel in the test area. The free-stream wall of the tunnel was adjusted for an approximate zero-pressure gradient, in the longitudinal direction as shown in figure 15 for $\beta = 0{\cdot}100$. Under these conditions the maximum variation in the two-dimensionality over a 24 in. span of the flow was less than 1 % at the jet exit and less than 1·3 % 90 slot widths downstream.

(b) Mean velocity and pressure measurements

Reference probes at $x' = 0$ in the wall-jet and the free stream were used to maintain constant flow conditions throughout the measurements. All mean velocities were computed from independent total and static pressure traverses of individual probes. A typical variation of static pressure in the lateral direction is shown in figure 15. The probes used were of the boundary-layer type, designed and tested for measurements near the wall. Although, as can be seen from figure 15, the static pressure varied substantially with x' in the development region of the jet,

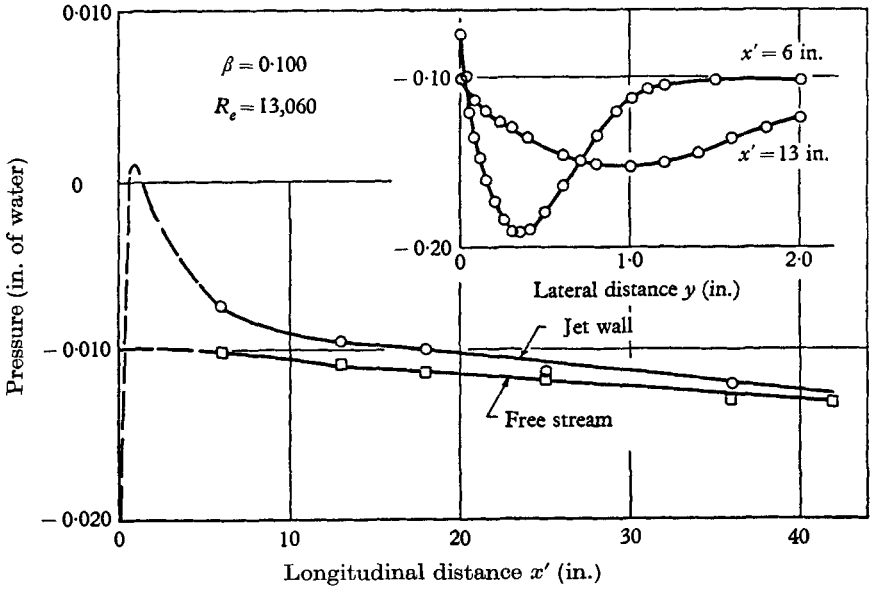

FIGURE 15. Static pressure distributions.

beyond $x' = 6$ in., or $x'/d_0 = 45{\cdot}8$, the longitudinal pressure gradient is essentially zero. In general, then, traverses were taken at $x'/d_0 = 45{\cdot}8$, 99·2, 137·4, 190·8 and 274·8. The pressures, when below 1·5 in. of water, were measured with an alcohol micromanometer of 0·0004 in. of water sensitivity; when above 1·5 in., with a precision inclined manometer. Mean velocity measurements in the immediate neighbourhood of the wall were made with a constant current hot-wire anemometer.

The wall shear was measured independently with a flattened Preston probe calibrated in a pipe. The details of this calibration are presented in a separate work by McGrew (1960). Head & Rechenberg (1962) have shown that for a given skin friction the Preston probe reading was the same for both a fully developed pipe and boundary-layer flow. The reliability of the data obtained for the wall shear is indicated in figure 4 which shows the fair matching of hot-wire and Preston probe results.

(c) Turbulence measurements

Turbulence measurements were taken with a multiple channel constant current hot-wire anemometer. The frequency response is reliable up to 100 kc/sec, but to eliminate noise, a matched 40 kc/sec filter was used in all measurements. Com-

pensation of the amplifier was achieved by the customary square-wave method. It was also checked by a phase-lag method which seems to be more precise but difficult to achieve in highly turbulent flows. The wires are of 0·00015 in. diameter tungsten 0·040 in. long and silver soldered to their supports. The wires were mounted with a slight slack in them as tight wires were found to vibrate in the flow. In addition, rubber cement was put on the coated portion of the wire and the supports to further dampen any vibrations. All measurements, except those in the immediate neighbourhood of the wall and those for the microscale, were conducted with an X-array with the wires about 0·008 in. apart. On many occasions identical measurements were made with a dual channel constant temperature set; the results were found to agree within the scatter which in some cases is about 10 %. The microscale was computed from measurements of the time rate of change of the instantaneous velocity.

4. Experimental results

The values of all characteristic flow quantities of the various velocity ratios investigated are listed in table 1.

(*a*) *Temporal mean velocity*

Figures 1 and 13 have already shown the experimental similarity in the inner and outer portions of the flow. Plots for β's other than 0·100 are as convincing but are not presented in this paper. Glauert's solution is given for the free-mixing region and agrees well with the experiments except at the outer edge of the flow where it diverges from the present results. This is to be expected as Glauert assumed a constant eddy viscosity for the whole free-mixing region, which is known to be invalid at the outer edge. For comparison, Tollmien's (1945) solution of the two-dimensional turbulent jet is also given on this figure.

As discussed in § 2, the maximum excess velocity ΔU_m decays as stated in (18), while the maximum velocity U_m can be approximated by (9). Experimental verification, including that of other investigators, is shown in figures 12 and 8. From the latter figure one can see that for higher β's the simple form of (7), describing the decay of U_m, is not entirely satisfactory. The growth of the outer characteristic half width $(\delta - \delta_1)$ is proportional to x_s, as indicated by (15), while the inner characteristic width δ_1 increases with x as given by (8). Figures 7 and 6 show all the present measurements in addition to those of many other experimenters for various velocity ratios β, including those for $\beta = 0$. It is clearly evident that the transformed co-ordinate x_s is able to reduce all results to the single linear equation (15). Thus, in allowing comparison for all β's, this reduced variable becomes a necessary tool.

The velocity profile at any x for a given β, U_0 and d_0 can be reconstructed as follows. The exponent a can be evaluated from (16). Equation (18) gives ΔU_m for a given x_s. For that same x_s, $(\delta - \delta_1)$ is given by (15). At this point, knowing the values of x_s, ΔU_m, the exponent a and U_s, (14) gives the location of x. Hence, δ_1 can be computed from (8). It must be remembered that U_m is best obtainable from ΔU_m and U_s. Considering the velocity similarity functions to be universal, then figures 1 and 13 at once give $U = f(x, y)$ for each similarity region.

x' (in.)	x_s (in.)	U_m (ft./sec)	ΔU_m (ft./sec)	U_τ^2 (ft./sec)^2	δ (in.)	δ_1 (in.)	δ_5 (in.)	$\overline{uv}_m$ (ft./sec)^2	$\overline{u}/U]_m$ (%)	$\overline{v}/U]_m$ (%)	δ_2 (in.)	δ_3 (in.)	δ_6 (in.)	δ_7 (in.)
$\beta = 0{\cdot}263$, $U_j = 217$ ft./sec, $x_0 = 0{\cdot}70$ in., $d_0 = 0{\cdot}131$ in., $a = -0{\cdot}850$														
6·0	4·8	141·8	81·8	53·5	0·32	0·065	0·74	92·5	16·8	10·8	0·25	0·050	0·40	0·43
13·0	8·6	110·8	53·2	25·9	0·58	0·127	1·30	49·5	12·5	8·7	0·39	0·077	0·55	0·65
18·0	10·6	99·1	41·3	20·8	0·76	0·173	1·61	27·1	10·4	7·6	0·52	0·147	0·70	0·83
18·0	10·7	100·6	42·2	21·5	0·77	0·185	1·67	31·8	12·4	8·8	0·64	0·163	0·74	0·80
25·0	13·4	91·9	34·0	16·2	0·99	0·267	2·16	22·9	10·1	7·4	0·85	0·210	0·91	1·10
36·0	16·6	84·1	26·0	12·8	1·31	0·381	2·86	14·5	8·4	5·9	1·05	0·355	1·06	1·27
$\beta = 0{\cdot}100$, $U_j = 217$ ft./sec, $x_0 = 1{\cdot}90$ in., $d_0 = 0{\cdot}131$ in., $a = -0{\cdot}670$														
6·0	7·1	124·0	104·4	39·4	0·50	0·073	1·25	116·0	32·3	22·8	0·35	0·070	0·70	0·73
13·0	12·8	90·1	71·1	19·7	0·93	0·150	2·16	69·2	25·4	18·0	0·70	0·102	1·16	1·20
18·0	16·4	79·3	58·6	14·7	1·19	0·202	2·97	48·0	25·4	17·8	0·90	0·165	1·48	1·76
25·0	21·2	69·8	48·2	11·0	1·53	0·294	3·56	40·9	23·2	16·0	1·12	0·160	1·76	2·15
36·0	27·6	60·2	37·1	7·9	2·06	0·373	4·90	34·4	20·7	17·0	1·59	0·230	2·27	2·52
$\beta = 0{\cdot}055$, $U_j = 414$ ft./sec, $x_0 = 1{\cdot}16$ in., $d_0 = 0{\cdot}131$ in., $a = -0{\cdot}540$														
6·0	6·8	243·5	225·7	161·3	0·49	0·070	1·48	601·3	44·0	31·2	0·36	0·035	0·73	0·87
13·0	13·3	177·4	161·8	67·2	0·95	0·120	2·50	316·5	44·0	32·0	0·67	0·110	1·45	1·73
18·0	17·7	148·7	132·2	55·5	1·28	0·174	3·42	222·9	46·4	35·2	0·96	0·150	2·01	2·20
25·0	24·6	128·1	116·7	37·4	1·69	0·229	4·50	186·1	—	—	1·41	0·160	—	—
36·0	35·5	104·3	97·0	26·3	2·47	0·394	6·20	136·4	—	—	1·90	0·145	—	—

x' (in.)	x_s (in.)	U_m (ft./sec)	ΔU_m (ft./sec)	U_τ^2 (ft./sec)^2	δ (in.)	δ_1 (in.)	δ_5 (in.)
$\beta = 0{\cdot}485$, $U_j = 134$ ft./sec, $x_0 = 0{\cdot}7$ in., $d_0 = 0{\cdot}099$–$0{\cdot}107$ in., $a = -1{\cdot}492$							
1·8	1·7	115·8	52·3	39·7	0·12	0·045	0·25
3·0	2·2	100·8	36·9	28·9	0·15	0·052	0·31
6·0	3·0	86·0	21·4	18·8	0·21	0·067	0·42
12·0	3·8	75·0	11·1	12·3	0·36	0·155	0·66
$\beta = 0{\cdot}274$, $U_j = 224$ ft./sec, $x_0 = 0{\cdot}7$ in., $d_0 = 0{\cdot}099$–$0{\cdot}105$ in., $a = -0{\cdot}895$							
3·0	2·7	152·5	91·6	58·1	0·21	0·058	0·48
6·0	4·4	126·1	63·0	35·8	0·32	0·071	0·71
12·0	7·2	99·5	40·3	22·1	0·55	0·141	1·27
17·0	8·8	94·3	32·2	17·3	0·65	0·188	1·55
24·0	11·2	87·1	26·6	13·6	0·90	0·266	2·06
36·4	13·5	83·1	19·3	—	1·05	0·284	2·55
48·2	16·1	74·5	15·4	—	1·47	0·511	3·27

x' (in.)	x_s (in.)	U_m (ft./sec)	ΔU_m (ft./sec)	U_τ^2 (ft./sec)^2	δ (in.)	δ_1 (in.)	δ_5 (in.)
$\beta = 0{\cdot}263$, $U_j = 117$ ft./sec, $x_0 = 0{\cdot}4$ in., $d_0 = 0{\cdot}131$ in., $a = -0{\cdot}859$							
6·0	4·6	74·5	42·6	—	0·37	0·085	—
13·0	8·0	58·7	26·2	—	0·66	0·154	—
18·0	10·3	52·8	21·4	—	0·87	0·216	—
25·0	13·1	48·4	17·7	—	1·13	0·310	—
36·0	16·5	44·4	13·7	—	1·47	0·436	—
$\beta = 0{\cdot}100$, $U_j = 210$ ft./sec, $x_0 = 1{\cdot}8$ in. $d_0 = 0{\cdot}117$–$0{\cdot}119$ in. $a = -0{\cdot}640$							
3·0	4·3	152·1	128·3	64·3	0·30	0·056	0·69
6·0	6·9	120·3	98·5	35·3	0·47	0·069	1·31
12·0	11·5	89·3	66·2	19·4	0·85	0·125	1·89
17·0	15·4	77·4	56·6	14·3	1·16	0·208	2·46
24·0	20·6	67·3	47·4	10·5	1·46	0·255	3·13
36·4	29·3	57·6	38·2	—	2·17	0·406	4·76
48·2	35·5	50·0	29·8	—	2·58	0·557	5·90

TABLE 1. Characteristic flow quantities in the jet.

The strong influence exerted by the free-mixing region upon the wall region becomes apparent in figure 16 which shows the universal velocity distribution in the immediate vicinity of the wall. Though a boundary-layer type similarity is demonstrated, the constants in

$$u/U_\tau = A \log (yU_\tau/\nu) + B$$

are different from the boundary-layer case as indicated on the graph, while the sublayer obeys the universal similarity form. It should be noted here that the effective opening of the Preston probe used was within the laminar sublayer and

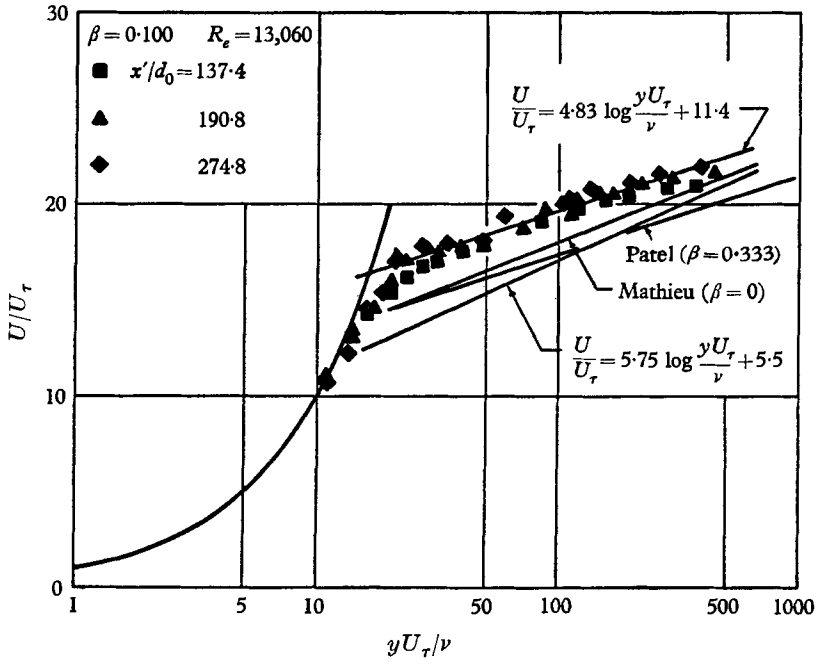

FIGURE 16. Law of the wall.

the buffer region. This figure also contains the data of Mathieu (1961) for his plane, 5 mm wide wall-jet inclined at an angle of 7 degrees to the wall and blowing at it from a distance of 200 mm. Mathieu did not find similarity in his case but, at the last station of $x = 500$ mm for which is effective x/d_0 cannot be calculated, his coefficients A and B begin to approach those of the present investigation. This indicates the possibility that the flow had not as yet become fully developed. The work of Patel further demonstrates the existence of similarity in this region; his results for $\beta = 0{\cdot}333$ are also given.

(*b*) *Shear stress*

Figure 17, giving experimental results of the wall shear, verifies the power-law form of (10). However, the exponents α obtained independently from the

maximum velocity (9) and the wall shear (10) are found to disagree at high β as shown on figure 8. Letting $f(\eta) = 1{\cdot}03\eta^{1/n}$, (10) and (11) become

$$u_\tau^2 = (1{\cdot}03)^2 cc_1^2 \frac{n(1-n\alpha)}{(n+1)(n+2)} \eta_3^{(1+2/n)} x^{-2\alpha},$$

$$c_f = 2(1{\cdot}03)^2 c \frac{n(1-n\alpha)}{(n+1)(n+2)} \eta_3^{(1+2/n)}.$$

Experimentally η_3 was determined by hot-wire measurements close to the wall, that is, by necessity only a few measurements. Due to the scarcity and difficulty of measurements a definite relation between η_3 and x cannot be established,

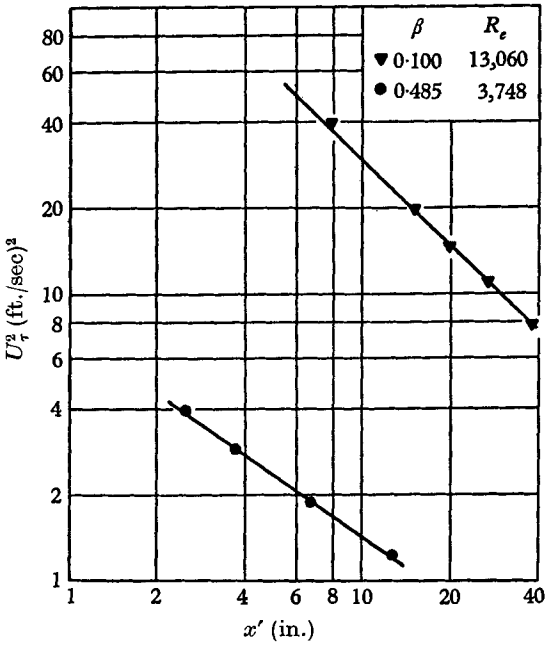

FIGURE 17. Wall shear distribution.

though it is certain that $\eta_3 < 1{\cdot}0$. The disagreement between exponents for the decay of the maximum velocity and wall shear at high β indicates a variation of η_3 with x. Similarly, figure 18 reveals that experimentally constancy of c_f with x is not maintained as predicted by (11) but that as in the boundary layer

$$c_f = c_4 R_i^m,$$

where R_i is the Reynolds number of the wall region, the coefficient c_5 and the exponent m vary with β as given on figure 18. The data of Mathieu & Tailland (1963), Bradshaw & Gee (1962) and Sigalla (1958) are also presented on this graph. It is seen that in the limit case of $\beta \to 0$ the present exponent m approaches that of Bradshaw for $\beta = 0$.

Figure 4, the non-dimensional shear distribution in the wall region, satisfies the relation of (6) within the scatter of hot-wire measurements. Thus similarity

in the inner layer exists in the shear distribution as well. It should be noted, however, that figure 4 gives the turbulent shear only. The exclusion of the laminar contribution, considering the relative magnitudes, is a valid approximation of the real situation.

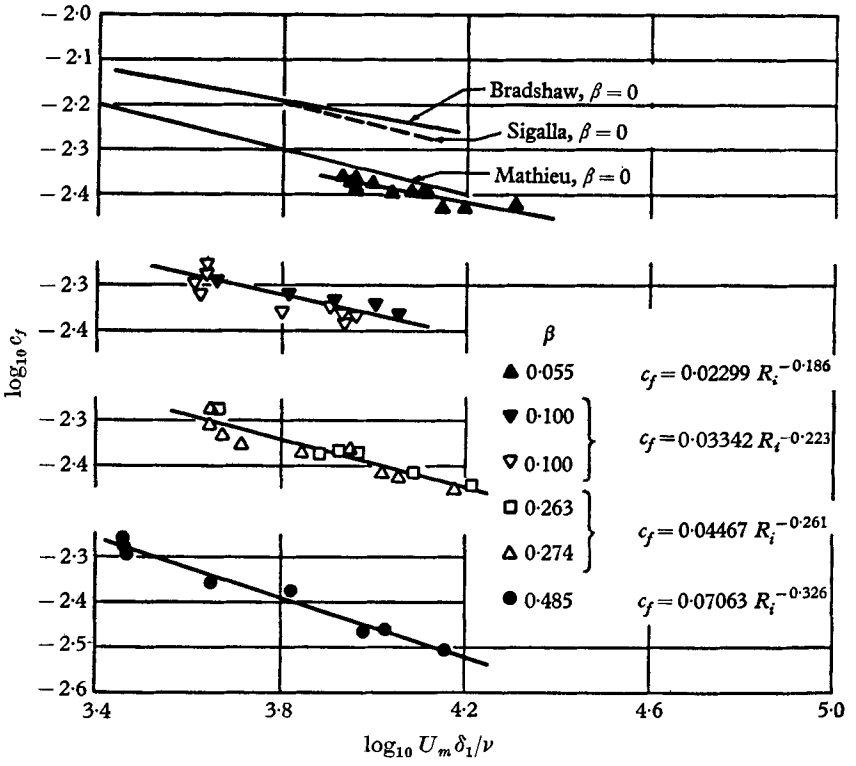

FIGURE 18. Variation of skin friction coefficient.

In the free-mixing region the maximum shear, as originally suggested by Förthmann (1936), is found to be the characteristic quantity for expressing the shear stress in a similarity form. Then, as figure 19 definitely indicated

$$\overline{uv} = \overline{uv}_m\, g_{12}(\xi_3), \tag{21}$$

where $\xi_3 = y - \delta_3/(\delta - \delta_3)$; that is, for turbulence terms, the flow is divided at δ_3, the point of zero shear. Schwarz & Cosart (1961) and others have used ΔU_m, or U_m for the case of zero free stream, as the characteristic term in place of $\overline{uv}_m$ in the above equation. While it is true, as figure 20 demonstrates, that $(\overline{uv}_m)^{\frac{1}{2}}$ is linear with ΔU_m, the intercept is non-zero. Therefore, it is not a simple matter of proportionality. This is not surprising as Corrsin (1943) in his round jet found that $(\overline{u}_m^2)^{\frac{1}{2}}/U_m$ was not constant for results which were taken up to 50 nozzle diameters downstream of the jet exit. From figure 20 in conjunction with equation (18) it is found that the maximum correlation

$$\overline{uv}_m = 1{\cdot}22 + 0{\cdot}00294 U_0 d_0 x_s^a/\nu. \tag{22}$$

Figure 21 shows the above equation in comparison with the experimental results for velocity ratio $\beta = 0{\cdot}263$, 0·100 and 0·055. Figure 22 displays the measured shear as well as the shear calculated from the integration of the Reynolds equation

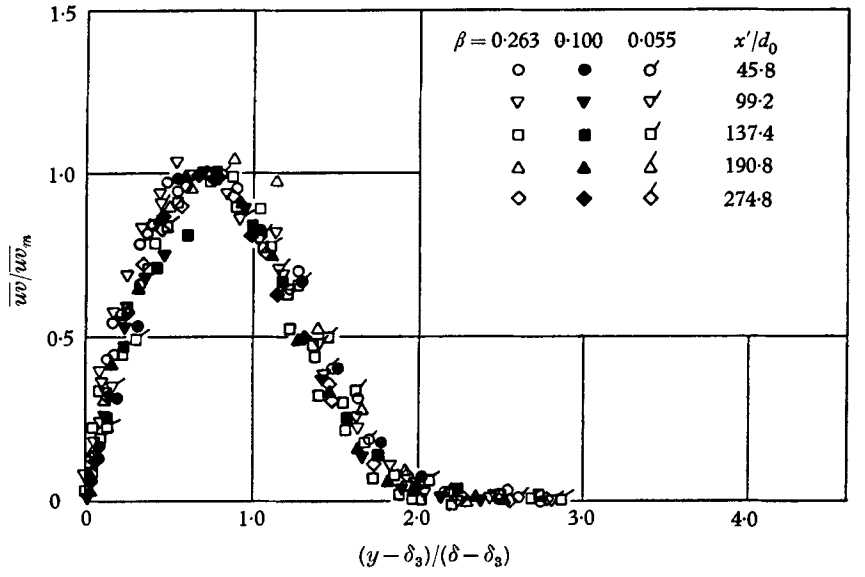

FIGURE 19. Similarity function of shear in outer region.

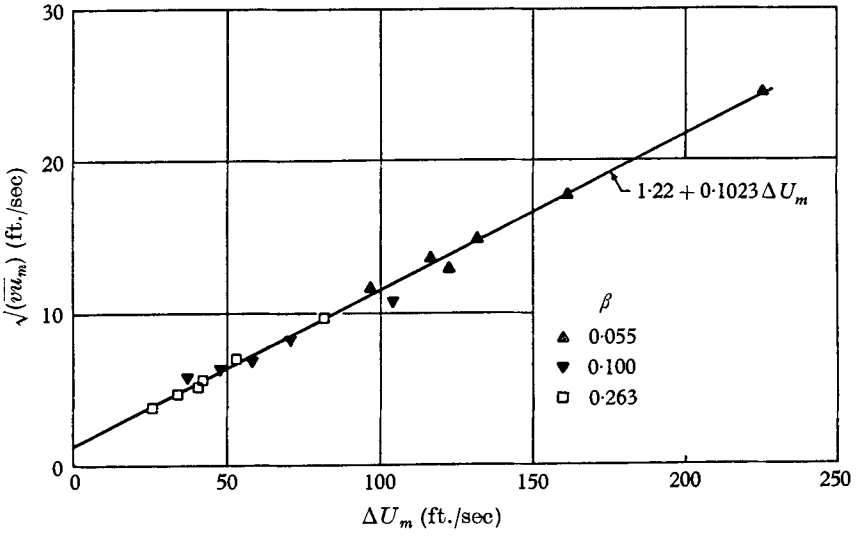

FIGURE 20. Characteristic velocity for the turbulence.

for one traverse at $\beta = 0{\cdot}263$. It is evident from all measurements and the above calculation that the location of zero shear point inside the flow always occurs on the side of the maximum velocity with the steepest gradient. This observation is discussed in detail in another paper.

(c) *Turbulence*

In the inner flow the temporal mean velocity and the correlation $\overline{uv}$ were found to display a boundary-layer type similarity when referred to the shearing velocity at the wall. From figure 5 one can also conclude that similarity also exists in the

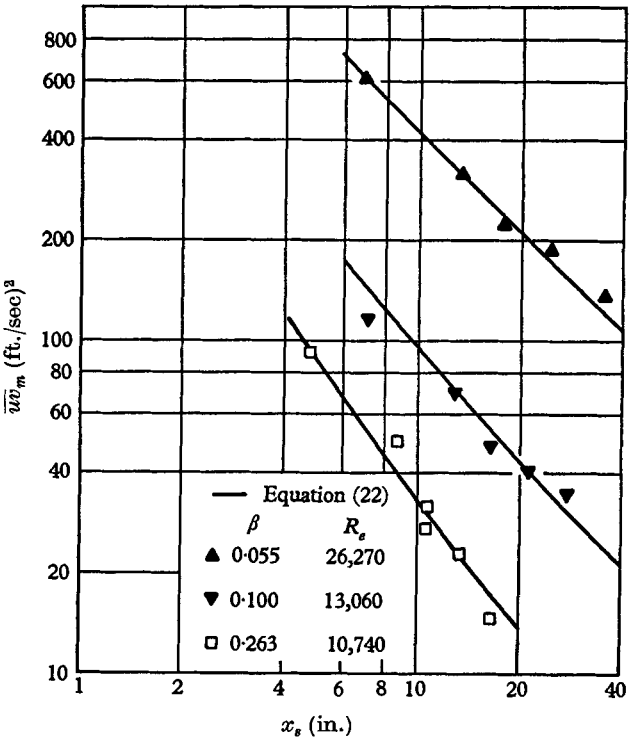

FIGURE 21. Decay of maximum shear.

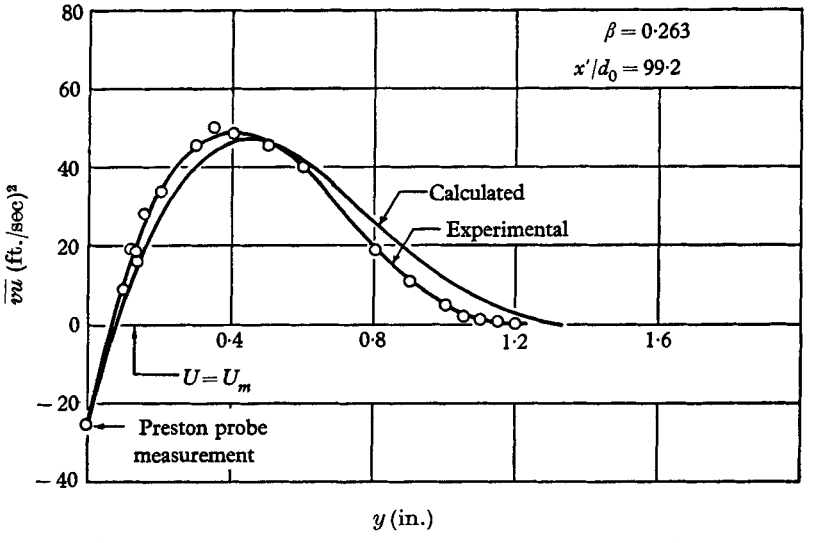

FIGURE 22. Comparison of measured and computed shear.

longitudinal turbulent velocity component u. In the outer region the turbulent velocities show fair similarity if the same characteristic scales are used as in the case of the shear; then

$$(\overline{u^2})^{\frac{1}{2}} = (\overline{uv}_m)^{\frac{1}{2}} g_1(\xi_3) \quad \text{and} \quad (\overline{v^2})^{\frac{1}{2}} = (\overline{uv}_m)^{\frac{1}{2}} g_2(\xi_3).$$

Figures 23 and 24 give the experimental results. The authors (1962*b*) showed the inadequacy of ΔU_m as the characteristic velocity.

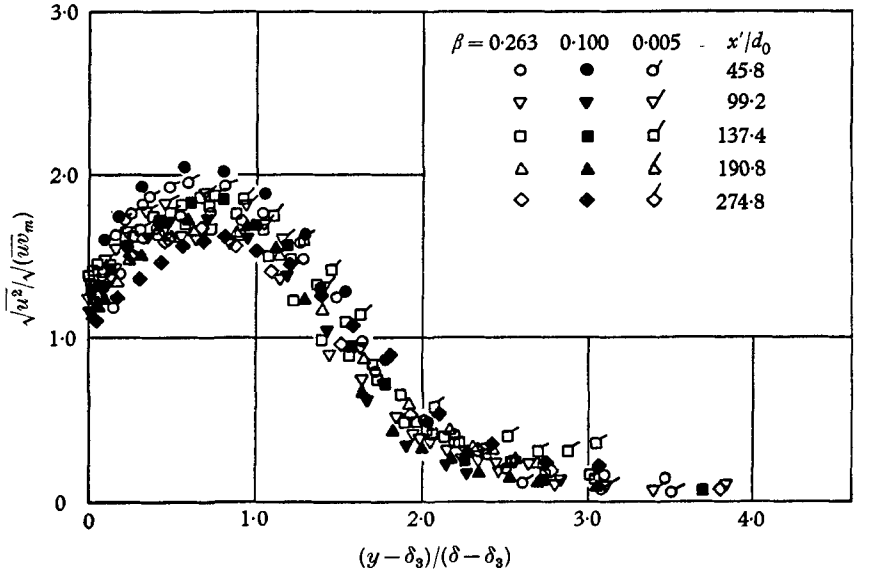

FIGURE 23. Turbulence similarity in outer region.

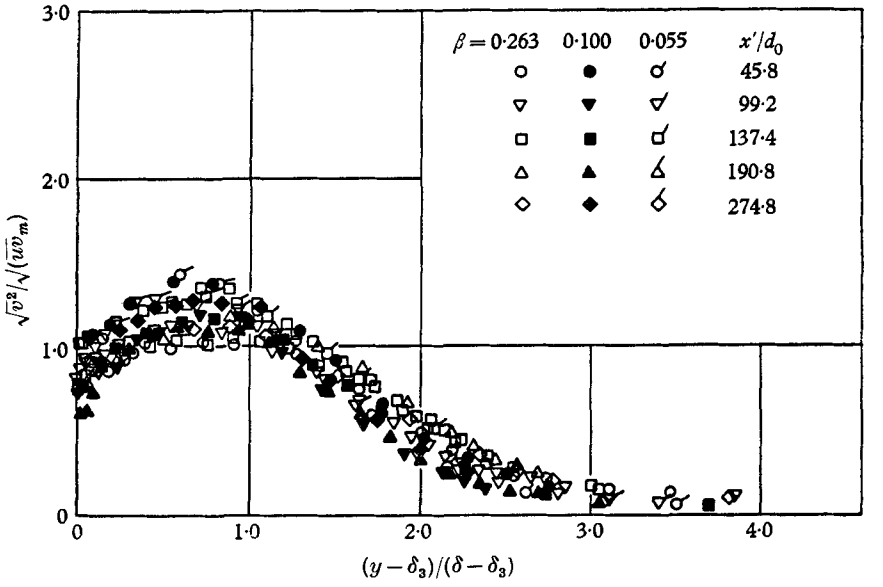

FIGURE 24. Turbulence similarity in outer region.

An interesting observation is shown on figure 25; the longitudinal microscale displays a depression in the region from the location of zero turbulent shear to that of maximum velocity.

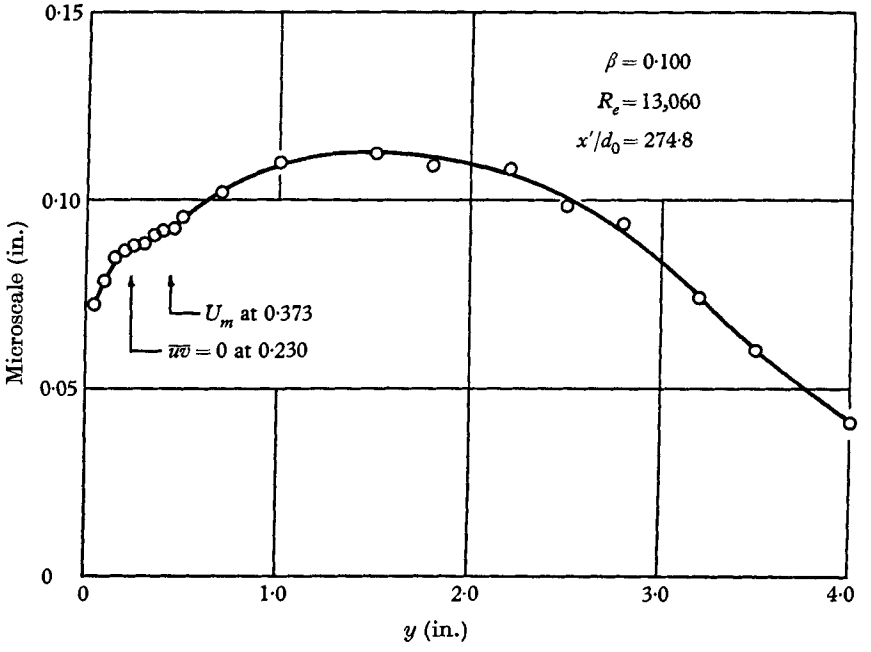

FIGURE 25. Microscale distribution.

5. Conclusions

Similarity was found to exist in both the inner and the outer layer for mean as well as turbulent quantities, however, the same scales do not apply to both layers. The flow was divided at the U_m location for mean measurements and at $\overline{uv} = 0$ for statistical quantities. This twofold partition was convenient in presenting the mean as well as the turbulent measurements. In any case, the separation between these two points is small.

In the inner layer the maximum velocity and its location were found to reduce the mean velocity to a similarity form independent of x. The width scale was found to vary as x for all β's. The corresponding boundary-layer width is proportional to $x^{\frac{1}{2}}$. The velocity scale varied as x to a power α where α is a function of the free stream to jet velocity ratio. In the immediate vicinity of the wall a universal boundary-layer type similarity exists, though the coefficients, as given by figure 16, have different values. The wall shearing velocity and location of $\overline{uv} = 0$ reduced $\overline{u}^2$ and $\overline{uv}$ to forms independent of x.

An expression for the wall shearing velocity is derived from which it can be seen that U_τ is proportional to U_m. Experimentally the friction coefficient is shown to be proportional to the inner Reynolds' number raised to a power, and consequently not constant with x.

In the outer layer a reduced longitudinal distance x_s is found necessary for comparing results at all β's. The use of the maximum excess velocity ΔU_m and the

characteristic half width of the free-mixing region $(\delta - \delta_1)$ for characteristic quantities gives experimental similarity for the mean velocities. Again the characteristic width is linear with x_s for all β's and the velocity scale varies as x_s^a, where the exponent a is a function of β. An empirical relation is given for the exponent a in terms of β, while the coefficient in the expression for ΔU_m is proportional to the exit excess Reynolds number. This then permits the complete reconstruction of the velocity profile at any x once the exit conditions are known.

The characteristic quantities for the turbulent velocities and the shear are the maximum shear and the half width $(\delta - \delta_3)$. It is definitely shown that the maximum excess velocity is not acceptable for the velocity scale here as ΔU_m is not proportional to the maximum shear. It is found, however, that there is a linear relation between the shear in the free-mixing region and the maximum excess velocity, thus permitting the calculation of the turbulent shear from mean measurements alone.

The authors gratefully acknowledge the Air Branch of the Office of Naval Research under whose sponsorship this work was undertaken. Mr Howard F. Hamm has taken active part in the experimentation and calculation.

REFERENCES

BRADSHAW, P. & GEE, M. T. 1962 Turbulent wall jets with and without an external stream, *Aero. Res. Counc., Lond., R & M*, no. 3252.

CORRSIN, S. 1943 Investigation of flow in an axially symmetrical heated jet of air. *NACA* ARC 3123.

EICHELBRENNER, E. A. & DUMARGUE, P. 1962 The problem of the plane turbulent wall-jet with an external flow of constant velocity. *J. Mecanique*, **1**, 109.

ESKINAZI, S. & KRUKA, V. 1962*a* Mixing of a turbulent wall-jet into a free stream. *Proc. Amer. Soc. Civil Engng*, **88**, 125.

ESKINAZI, S. & KRUKA, V. 1962*b* Turbulence measurements in a two-dimensional wall-jet with longitudinal free stream. *Syracuse Univ. Res. Inst. Rep.* ME 937–6205P.

ESKINAZI, S. & YEH, H. 1956 An investigation on fully developed turbulent flows in a curved channel. *J. Aero. Sci.* **23**, 23.

FÖRTHMANN, E. 1936 Turbulent jet expansion. *NACA* TM-789.

GEORGE, A. R. 1959 An investigation of a wall jet in a free stream. *Princeton Univ. Rep.* no. 479.

GLAUERT, M. B. 1956 The wall jet. *J. Fluid Mech.* **1**, 625.

HEAD, M. R. & RECHENBERG, I. 1962 The Preston tube as a means of measuring skin friction. *J. Fluid Mech.* **14**, 1.

LIEPMANN, H. W. & LAUFER, J. 1947 Investigations of free turbulent mixing. *NACA TN* 1257.

MATHIEU, J. 1959 Evolution d'un jet plan frappant sous une incidence de 7° une plaque plan lisse. *C.R. Acad. Sci.* **248**, 2713.

MATHIEU, J. 1961 Contribution a l'étude aerothermique d'un jet plan evoluant en presence d'une paroi. *Publ. Sci. Tech. Ministere de L'Air*, no. 374.

MATHIEU, J. & TAILLAND, A. 1961 Etude d'un jet plan dirigé tangentiellement a une paroi. *C.R. Acad. Sci.* **252**, 3736.

MATHIEU, J. & TAILLAND, A. 1963 Etude d'un jet plan dirigé tangentiellement a une paroi. *C.R. Acad. Sci.* **256**, 2768.

MCGREW, J. 1960 The effect of probe geometry in the determination of skin friction by means of pitot tubes. *Master's Thesis, Syracuse Univ.*

MYERS, G. E., SCHAUER, J. J. & EUSTIS, R. H. 1961 The plane turbulent wall jet. *Stanford Univ. Mech. Engng Dept. Rep.* no. 1.

PATEL, R. P. 1962 Self preserving two-dimensional turbulent jets and wall jets in a moving stream. *Master's Thesis, McGill Univ.*

PATEL, R. P. & NEWMAN, B. G. 1961 Self preserving two-dimensional jets and wall jets in a moving stream. *McGill Univ. Rep.* Ae 5.

SCHWARZ, W. H. & COSART, W. P. 1961 The two-dimensional turbulent wall-jet. *J. Fluid Mech.* **10**, 481.

SIGALLA, A. 1958 Measurements of skin friction in a plane turbulent wall jet. *Journal of the Royal Aeronautical Society*, **62**, 873.

THOMAS, F. 1962 Untersuchungen uber die grenzschicht Stromawarts von einem Ausblasespalt. *Deut. Forshungsanstalt, Luft. und Raumfahrt*, no. 168.

TOLLMIEN, W. 1945 Calculation of turbulent expansion processes. *NACA* TM-1085.

TOWNSEND, A. A. 1956 *The structure of turbulent shear flow.* Cambridge University Press.

VERHOFF, A. 1963 The two-dimensional turbulent wall jet with and without an external free stream. *Princeton Univ. Rep.* no. 626.